Alloying at Surfaces by the Migration of Reactive Two-Dimensional Islands

A. K. Schmid, N. C. Bartelt, R. Q. Hwang

We have studied the formation kinetics of the copper-tin alloy bronze when tin is deposited on the (111) surface of copper at room temperature. Low-energy electron microscopy and atomic-resolution scanning tunneling microscopy reveal that bronze forms on the surface by a complicated, unanticipated cooperative mechanism: Ordered two-dimensional tin islands containing several hundred thousand atoms spontaneously sweep across the surface, leaving bronze alloys in their tracks. We propose that this process, driven by surface free energy, is a version of the "camphor dance" observed on liquid surfaces, and should be a general mechanism of surface alloying when surface diffusion is faster than exchange into the substrate.

Our present ability to develop high-performance alloys depends on the understanding of the processes of atomic diffusion by which they form. Recently, alloys have been discovered that exist only on surfaces and do not have bulk counterparts (*1, 2*). Because controlling the nanoscale structure of these alloys offers a way to manipulate the chemical (*3*) and magnetic properties (*4*) of surfaces, it is important to determine the atomic processes responsible for their formation. Images of the static structure of surface alloys have shown that the mechanisms of surface alloying can be much different and more complicated than in the bulk (*5*). However, the precise sequence of atomic events occurring during surface alloying is usually unknown.

Recent progress in real-time microscopy techniques allows the observation of the time dependence of surface structure in unprecedented detail. Here, we used low-energy electron microscopy (LEEM) (*6*) and atomic-resolution scanning tunneling microscopy (STM) to study in real time the formation of bronze (Cu-Sn) when Sn is deposited on Cu(111). The alloying occurs by a striking, completely unanticipated cooperative process. We observe that shortly after deposition of Sn on Cu(111), two-dimensional (2D) Sn crystals containing several hundred thousand atoms coalesce on the surface. These crystalline islands proceed to move spontaneously along the surface in a systematic fashion. As the islands move, Sn atoms within the islands randomly exchange with Cu atoms in the surface. The exchanged Cu atoms are ejected from the Sn islands in the form of ordered 2D bronze crystals. We have traced the driving force of the remarkable motion of the Sn islands to simple atomic interactions: Sn atoms on top of the Cu surface are strongly repelled by Sn atoms already incorporated into the Cu. The islands thus lower the surface free energy by moving toward unalloyed regions of the surface.

Before discussing our experiments in detail, we point out some general features of the Sn-Cu system. Because Sn atoms are bigger than Cu atoms, they are incorporated into bulk copper only with difficulty: The room-temperature equilibrium solubility of Sn in Cu is low. However, Sn atoms can be relatively easily incorporated into the top atomic plane of the Cu(111) surface, where the size mismatch is readily accommodated by out-of-plane displacements. It is thus not surprising (*2*) that Sn atoms in single-crystal copper samples segregate to (111) surfaces in the form of $(\sqrt{3}\times\sqrt{3})R30°$ ordered surface alloy with one Sn atom for every two Cu atoms (*7, 8*). To form such surface phases by Sn deposition, Sn atoms must exchange into the Cu surface. For the Sn-Cu system, this process appears to be much more difficult than Sn diffusion on the surface, which leads to the surprisingly complex process mentioned above.

Figure 1A (*9*) shows a LEEM image of a

Sandia National Laboratories, Livermore, CA 94551, USA.

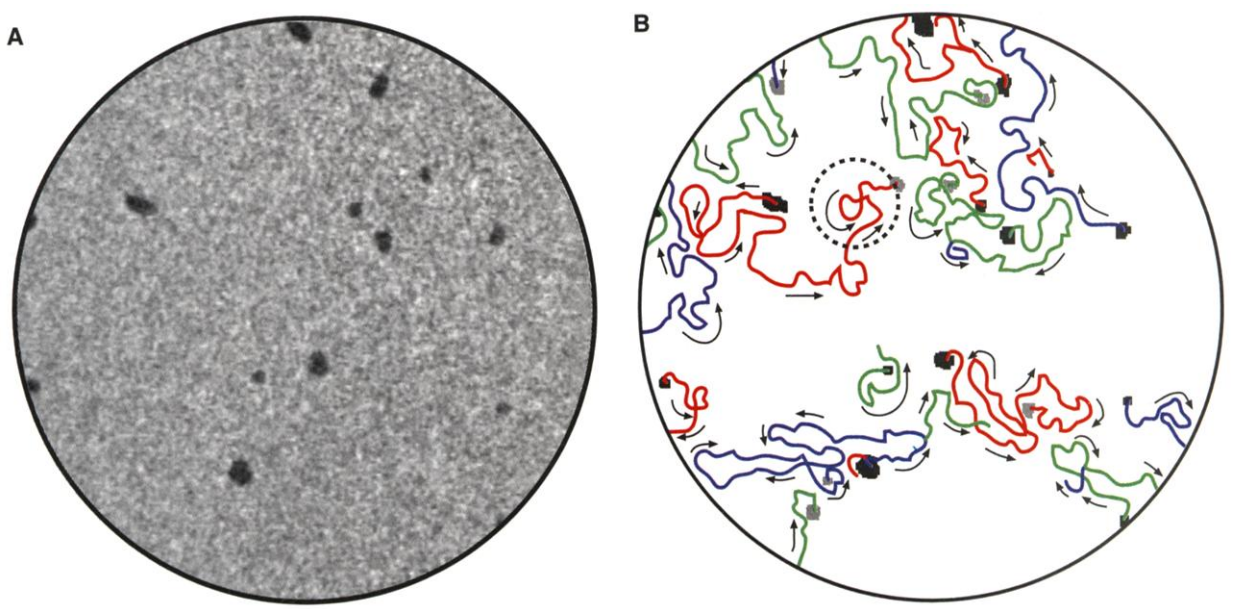

Fig. 1. LEEM images (1.5 μm across) of mobile 2D islands on Cu(111). **(A)** Sn islands (dark) formed during Sn deposition on a clean Cu(111) surface (bright background) at 290 K. This image was formed using 25-eV specularly reflected electrons. To highlight the self-avoiding nature of the trajectories, **(B)** shows the trajectories of these islands during the next 10 min. The circled segment of a trajectory shows an example of an island "painting itself into a corner," driving it to cross its own track. The initial islands are black; the (smaller) final islands are indicated in gray.

Cu(111) surface (field of view, 1.5 μm) after ~0.02 monolayers of Sn have been deposited (*10*) in ultrahigh vacuum at 290 K. Within 2 s, the Sn has coalesced into 2D islands with diameters on the order of 100 nm. Separate STM and low-energy electron diffraction experiments show that these 2D islands are well ordered with a (2×2) unit cell. Recording LEEM images at a rate of 30 per second revealed that the Sn islands move across the surface (Fig. 1B). As the islands move, they occasionally leave behind smaller immobile objects. Smaller scale images of these objects in the wake of a moving Sn island are shown in Fig. 2 (*9*). The speed of the islands is fairly constant, as shown by the record of the positions of the centers of mass of the islands (plotted in Fig. 2B) or by the superimposition of the positions of the islands (Fig. 2C). The total area of the Sn islands gradually diminishes with time. After a few minutes, all of the islands have dissolved, leaving only the smaller, comparatively static, features distributed across the surface.

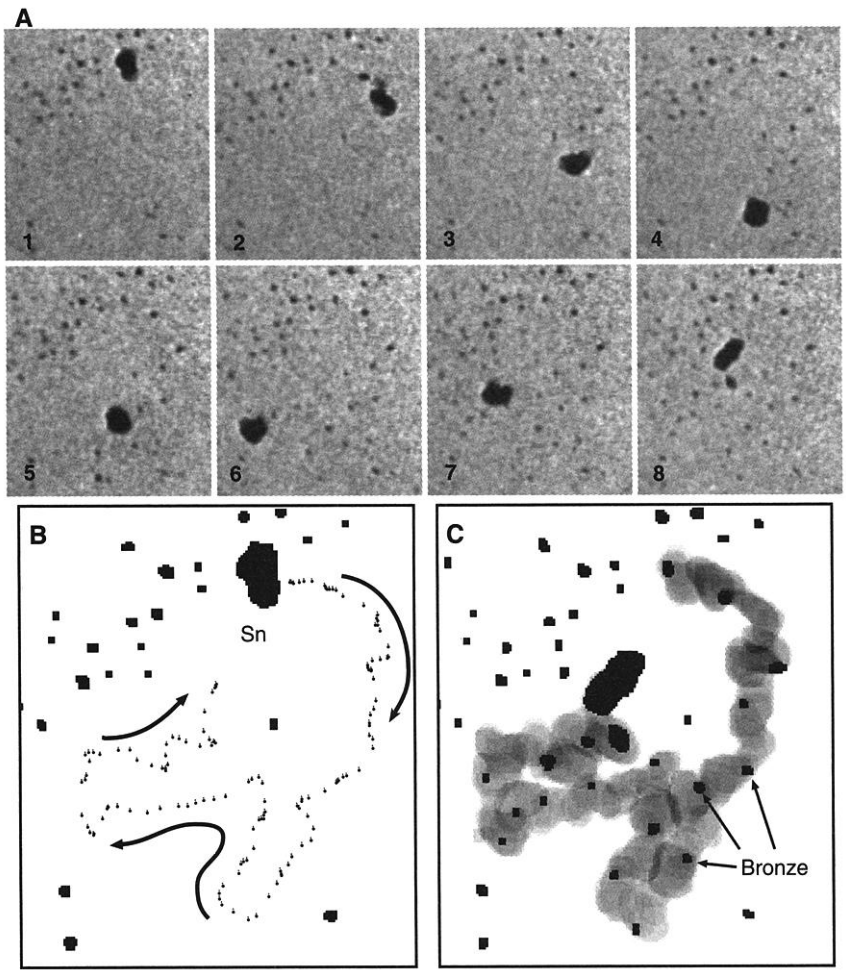

Fig. 2. (**A**) Sequence of LEEM images (0.6 μm wide) of a Sn island running on a Cu(111) surface at 290 K. The time between images is 36 s. The large black object is the Sn island; the small static dark objects are ordered bronze islands that have been ejected from the Sn island. (**B**) The trajectory of the center of mass of this island. (**C**) Superimposition of the intermediate positions of the islands; the gray level indicates how long the Sn island was over each position on the surface.

Atomic-scale STM images taken during and after this process provide clues for an atomic-level explanation of what is occurring during this motion. Figure 3 shows STM images of the surface taken half an hour after deposition. The first notable features of these images are islands one atomic layer in height (Fig. 3, D and E), consisting of the previously anticipated $(\sqrt{3}\times\sqrt{3})R30°$ phase. We identify these surface bronze islands as the static features left behind by the moving Sn islands observed with LEEM. Surrounding these islands, STM reveals a rather random arrangement of Sn atoms incorporated into the Cu surface. These incorporated Sn atoms lie in tracks (Fig. 3E) that presumably mark the previous passage of a Sn island. The number of randomly incorporated Sn atoms is consistent with the area of the bronze islands, given that each $(\sqrt{3}\times\sqrt{3})R30°$ unit cell contains two exchanged Cu atoms. Another notable feature of these STM images is the clouds of random "streaks" over the unalloyed Cu surface (Fig. 3B). This sort of noise is characteristic of atoms moving rapidly under the STM tip while it is scanning. We interpret

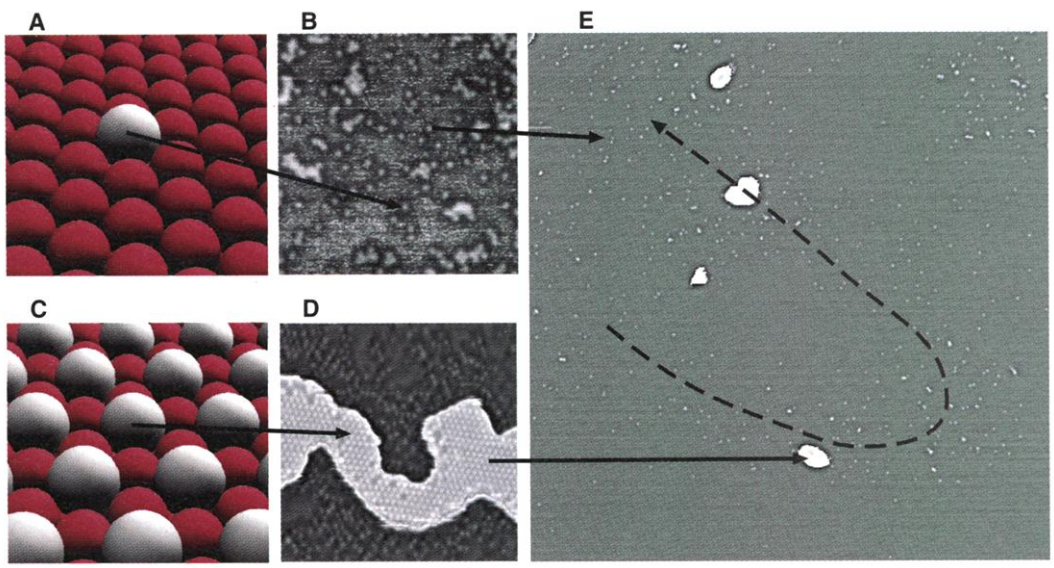

Fig. 3. (**A** and **C**) Schematic atomic configurations, and (**B** and **D**) atomic-resolution (15 nm by 15 nm) STM images, of bronze formation several hours after Sn deposition on the Cu(111) surface. The white spots in (B) are single Sn atoms embedded in the top layer of the Cu crystal, as suggested in the schematic in (A) where the Cu atoms are red and the larger Sn atom is white. (D) An STM image of the $(\sqrt{3}\times\sqrt{3})R30°$ structure of the ordered atomic layer islands, as shown schematically in (C). In (**E**), a 250 nm by 250 nm STM image shows the alloyed regions in the track of a Sn island that has passed through the field of view, leaving behind the (bright) immobile bronze islands. [Panels (B) and (D) are only representative of the corresponding regions indicated in (E).]

this noise as a dilute 2D gas of Sn atoms diffusing across the surface. This dilute gas persists for several days after Sn deposition. The lattice gas appears to strongly avoid regions near incorporated Sn. The large mobile Sn islands are also observable in other STM scans taken during Sn deposition, and these images confirm the (2×2) order. The islands are observed before any alloying is detected, confirming that they are primarily composed of Sn. The islands are too mobile to track on the several-minute acquisition time of STM images—a problem one usually associates with single atoms, not ordered islands containing 100,000 atoms!

The combined STM and LEEM observations suggest the following mechanism for surface bronze formation. The fact that Sn islands form within 2 s during deposition, before appreciable alloying occurs, indicates that the energetic barrier for exchange of a Sn adatom with a Cu surface atom is much higher than that for Sn diffusion. The stability of the Sn islands and lattice gas over clean Cu, and the absence of Sn from large areas of the Cu surface (Fig. 3E), provide further evidence for a relatively high exchange barrier. When exchange does occur, the tracks of exchanged Sn in Fig. 3E show that it is more probable in the dense Sn islands (*11*) and leads to Cu incorporation into the Sn islands. When the density of Cu in the islands becomes sufficiently large, ordered bronze islands are nucleated. These islands are relatively static and are left behind when the Sn islands move.

To understand the engine for the island motion, we first note that if there were a repulsion of diffusing Sn with incorporated Sn, then the surface free energy would be greater when a Sn island is over the random bronze alloy than when it is over clean Cu. There would then be a clear energetic driving force for the consistent motion of Sn islands away from their path. Several pieces of evidence indicate that this repulsion exists and causes the island motion. First, the repulsion would imply that a traveling Sn island would avoid the track of itself or of other islands. Inspection of the trajectories in Figs. 1 and 2 shows this to be true: When islands meet a track, they change direction if that allows them to move over unalloyed regions. An island will cross a track if it cannot avoid it by changing direction. An example of this is shown in the circled region of Fig. 1B, where an island has "painted itself into a corner." After tracing the motion of hundreds of islands, we observed nonforced track-crossing events only rarely; the one example slightly below the center of Fig. 1B was associated with a small island that completely dissolved soon after. Further evidence for the repulsion comes from first-principles electronic structure calculations of the interaction of Sn with incorporated Sn (*12*) and the repulsion between the incorporated Sn and the Sn lattice gas shown in Fig. 3B.

The island trajectories are not similar to the trajectories of islands undergoing the thermal Brownian motion that has been observed for much smaller islands on metal surfaces (*13–16*); in this case, motion would be uncorrelated from time to time. We observe, however, that there is a clear tendency for islands to continue to move in the same direction.

To be more quantitative about this idea of surface tension–driven island motion, we can compare the observed velocities with standard theories of island motion. The problem is to compute the steady-state velocity that characterizes island motion. Generally, the velocity v of the islands will be proportional to the thermodynamic driving force F applied to it,

$$v = \mu(R)F \qquad (1)$$

where R is the island radius and $\mu(R)$ is the island mobility, which depends on the mechanism of diffusion. F is proportional to the difference between the surface free energy of Sn covering the dilute Sn alloy and that of Sn covering clean Cu. Because of the random nature of the dilute Sn alloy, it is reasonable to suppose this free energy difference to be proportional to the density of incorporated Sn. Thus,

$$F = \varepsilon \int_{-R}^{R} \rho(y)dy \qquad (2)$$

where ε is the free energy cost of having a single Sn atom under the island, and $\rho(y)$ is the atomic density of the incorporated Sn just behind the island (Fig. 4). Given the random exchange mechanism, the amount of incorporated Sn is proportional to the time $t(y)$ the island was over each region of the surface, so $\rho(y) = \beta t(y) = 2\beta(R^2 - y^2)^{1/2}/v$, assuming circular islands and a constant alloying rate β. Thus, $F = \varepsilon\beta\pi R^2/v$. Substituting this expression into Eq. 1 yields a self-consistent requirement for the steady-state velocity of the island as a function of radius,

$$v(R) = [\pi\mu(R)\varepsilon\beta]^{1/2}R \qquad (3)$$

Further analysis shows that this steady state is stable: Perturbations in the island's motion (caused by obstacles in its path or by the emission of a bronze island, for instance) would quickly relax back to the steady state. This relaxation was often observed experimentally.

A way to evaluate the applicability of this interpretation is to compare the predicted size dependence of the velocity with experiment. As seen in Fig. 5A, the measured velocities are approximately independent of R. From Eq. 3, the dependence of velocity on R in our model depends on how the mobility μ varies with R, which is determined by how mass is transported within the island during its motion. If there are atomic currents through islands (caused by vacancy diffusion, for example), $\mu(R)$ is easily shown (*17*) to be equal to $\omega^2 D_d \rho_d/(\pi k_B T R^2)$, where ω is the atomic area, D_d is the diffusion coefficient of the diffusing species, ρ_d is the density of the diffusing species, k_B is the Boltzmann constant, and T is absolute temperature. This inverse-square dependence on R leads to a size-independent island velocity, as observed, equal to $(D_d\rho_d\omega^2\varepsilon\beta/k_BT)^{1/2}$. If there were

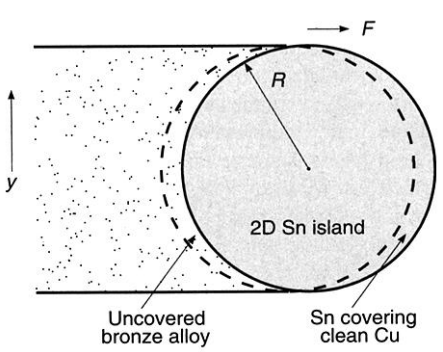

Fig. 4. Schematic showing the source of the force F on a Sn island. By moving to the right, the island uncovers a bronze alloyed surface and covers clean Cu, lowering the surface free energy.

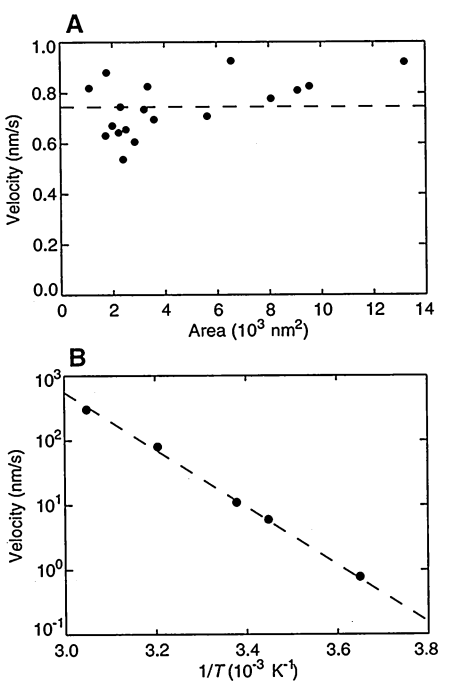

Fig. 5. Analysis of Sn island motion. (**A**) Plot of the average island velocity versus island area at 270 K, showing that the velocity is approximately independent of size. The dashed line indicates the average velocity. (**B**) Arrhenius plot of the island velocity; the slope of the dashed line corresponds to an activation energy of 900 meV.

only currents of Sn atoms around the edge of the island, then $\mu(R)$ would drop rapidly with island size, proportional to $1/R^3$ (*17*), and give a $v(R)$ that would increase with decreasing radius as $1/\sqrt{R}$. Thus, as long as D_d is nonzero, diffusion through the islands for sufficiently large R values should provide the dominant contribution to their mobility, consistent with our observations.

We can experimentally adjust the speed of the islands over several orders of magnitude by changing the temperature slightly around room temperature. In an Arrhenius plot of the velocity (Fig. 5B), the linearity suggests that the processes responsible for the island motion are activated with an energy of 900 meV. From the above analysis, this should be half of the activation energy associated with the product $D_d\rho_d\beta$. Because diffusion barriers, defect formation energies, and exchange energies are typically on the order of hundreds of meV, the activation energy we measure is reasonable within this model. From our measurements at 270 K, we find that the Sn-Cu exchange rate is roughly one atom per 4000 s. Assuming a value of ε on the order of 100 meV, typical diffusion prefactors on the order of 10^{12} s^{-1}, and the experimentally measured activation energy, we find that $(D_d\rho_d\omega^2\varepsilon\beta/k_BT)^{1/2}$ yields island velocities of the observed order of magnitude. So the simple picture of Fig. 4 seems to be consistent with everything we know at present about this system. Given the simplicity of the driving force for the motion of the reactive Sn islands, this mechanism of surface alloying might be expected to be common when surface diffusion is faster than exchange into the substrate.

We make three comments about the surface bronze formation: (i) The trajectories shown in Figs. 1 and 2 do not convey the full animation of the Sn island motion (*9*); the Sn islands often appear to react to their surroundings in a complex way (pausing when their best path is not obvious, for example) and are efficient in finding new unalloyed regions. It is interesting that such complexity can arise from such a seemingly simple situation as surface alloying. (ii) Surface free energy–driven motion of particles on liquid surfaces (or liquids on solid surfaces) is a familiar phenomenon (*18–24*); the observation of the similar motion of camphor particles across water dates to 1686 (*23, 24*) and was the subject of much discussion in the 19th century. It allowed Lord Rayleigh to estimate molecular dimensions and motivated him to perform an accurate determination of the surface tension of water (*25*), for example, and now reappears in the context of solids on the nanoscale. (iii) Control of the island motion presents the possibility of manipulation of surface alloy formation to create useful and novel nanoscale structures.

References and Notes

1. L. P. Nielsen *et al.*, *Phys. Rev. Lett.* **71**, 754 (1993).
2. A. Christensen *et al.*, *Phys. Rev. B* **56**, 5822 (1997).
3. F. Besenbacher *et al.*, *Science* **279**, 1913 (1998).
4. S. S. P. Parkin, *Annu. Rev. Mat. Sci.* **25**, 357 (1995).
5. See, for instance, A. K. Schmid, J. C. Hamilton, N. C. Bartelt, R. Q. Hwang, *Phys. Rev. Lett.* **77**, 2977 (1996).
6. E. Bauer, *Rep. Prog. Phys.* **57**, 895 (1994).
7. J. Erlewein, S. Hofmann, *Surf. Sci.* **68**, 71 (1977).
8. G. Contini, V. Di Castro, N. Motta, A. Scarlata, *Surf. Sci.* **405**, L509 (1998).
9. For movies of the motion of the islands in Figs. 1 and 2, see *Science* Online (www.sciencemag.org/cgi/content/full/290/5496/1561/DC1).
10. For convenience, our Cu crystals were grown as films on a Ru substrate. The films were more than 20 atomic layers thick, and the spacing between surface atomic steps was often several micrometers. Precise x-ray crystallography measurements show that the lattice spacing of these crystals is indistinguishable from that of bulk Cu [H. Zajonz, D. Gibbs, A. P. Baddorf, V. Jahns, D. M. Zehner, *Surf. Sci.* **447**, L141 (2000)].
11. Evidence for Sn-Cu exchange within islands rather than at island edges comes from experiments in which we completely covered the surface with the (2×2) Sn phase. Despite the absence of island edges, the rate of creation of the $(\sqrt{3}\times\sqrt{3})R30°$ alloy phase was identical to the observed rate for islands.
12. N. C. Bartelt, in preparation.
13. J. M. Wen, S. L. Chang, J. W. Burnett, J. W. Evans, P. A. Thiel, *Phys. Rev. Lett.* **73**, 2591 (1994).
14. K. Morgenstern, G. Rosenfeld, B. Poelsema, G. Comsa, *Phys. Rev. Lett.* **74**, 2058 (1995).
15. S. C. Wang, G. Ehrlich, *Phys. Rev. Lett.* **79**, 4234 (1997).
16. W. W. Pai, A. K. Swan, Z. Y. Zhang, J. F. Wendelken, *Phys. Rev. Lett.* **79**, 3210 (1997).
17. S. V. Khare, N. C. Bartelt, T. L. Einstein, *Phys. Rev. Lett.* **75**, 2148 (1995).
18. F. D. Dos Santos, T. Ondarcuhu, *Phys. Rev. Lett.* **75**, 2972 (1995).
19. C. D. Bain, G. D. Burnett-Hall, R. R. Montgomerie, *Nature* **372**, 414 (1994).
20. M. K. Chaudhury, G. M. Whitesides, *Science* **256**, 1539 (1992).
21. F. Brochard, *Langmuir* **5**, 432 (1989).
22. P. G. de Gennes, *Physics A* **249**, 196 (1998).
23. L. E. Scriven, C. V. Sternling, *Nature* **187**, 186 (1960).
24. A. W. Adamson, *Physical Chemistry of Surfaces* (Wiley, New York, ed. 4, 1982), pp. 97–116.
25. Lord Rayleigh, *Philos. Mag.* **30**, 386 (1890).

26. Supported by the Office of Basic Energy Sciences, Division of Materials Sciences, U.S. Department of Energy, under contract DE-AC04-94AL85000.

10 July 2000; accepted 26 September 2000

High Shear Strain of Olivine Aggregates: Rheological and Seismic Consequences

M. Bystricky,* K. Kunze, L. Burlini, J.-P. Burg

High-pressure and high-temperature torsion experiments on olivine aggregates in dislocation creep show about 15 to 20% strain weakening before steady-state behavior, characterized by subgrain-rotation recrystallization and a strong lattice preferred orientation. Such weakening may provide a way to focus flow in the upper mantle without a change in deformation mechanism. Flow laws derived from low strain data may not be appropriate for use in modeling high strain regions. In such areas, seismic wave propagation will be anisotropic with an axis of approximate rotational symmetry about the shear direction. In contrast to current thinking, the anisotropy will not indicate the orientation of the shear plane in highly strained, recrystallized olivine-rich rocks.

Seismic anisotropy in oceanic and continental lithospheres is commonly attributed to deformation-induced lattice preferred orientations (LPOs) of olivine and pyroxene (*1–6*) and is used to determine flow patterns in the upper mantle (*7, 8*). To give weight to this interpretation, we must understand how olivine LPOs develop and evolve with strain in particular deformation settings. Flow in the mantle involves high strain and non-coaxial deformation, but most experimental studies on polycrystalline olivine have been performed under uniaxial compression, in which deformation is coaxial and the total amount of strain (equivalent strains <0.5) is limited (*9–12*). Olivine samples deformed to shear strains up to 1.5 using a diagonal-cut assembly (*13, 14*) yielded useful microstructural and textural observations. However, these experiments may not have produced steady-state deformation textures. In addition, such an experimental arrangement does not allow a detailed rheological study, because combined compressional and simple shear components contribute to the deformation and because the state of stress is poorly known at high strains (*15*). Here we present results on the experimental deformation of olivine aggregates in torsion yielding bulk shear strains up to $\gamma = 5$. The aim of this study was to achieve non-coaxial deformation and to investigate the detailed microstructural, textural, and rheological evolution of polycrystalline olivine over a larger strain range than previously accessible.

Olivine aggregates were hot-pressed from San Carlos olivine powders (*16*). Deformation experiments were carried out in a high-

Geologisches Institut, ETH-Zentrum, 8092 Zürich, Switzerland.

*To whom correspondence should be addressed. E-mail: misha@erdw.ethz.ch